nature communications

Article

https://doi.org/10.1038/s41467-023-40135-x

Enhancing reactivity of SiO^+ ions by controlled excitation to extreme rotational states

Received: 17 September 2022

Accepted: 11 July 2023

Published online: 24 July 2023

Check for updates

Sruthi Venkataramanababu[1,2], Anyang Li[3] ✉, Ivan O. Antonov[4], James B. Dragan[2], Patrick R. Stollenwerk[5], Hua Guo[6] & Brian C. Odom[2] ✉

Optical pumping of molecules provides unique opportunities for control of chemical reactions at a wide range of rotational energies. This work reports a chemical reaction with extreme rotational excitation of a reactant and its kinetic characterization. We investigate the chemical reactivity for the hydrogen abstraction reaction $SiO^+ + H_2 \rightarrow SiOH^+ + H$ in an ion trap. The SiO^+ cations are prepared in a narrow rotational state distribution, including super-rotor states with rotational quantum number (j) as high as 170, using a broad-band optical pumping method. We show that the super-rotor states of SiO^+ substantially enhance the reaction rate, a trend reproduced by complementary theoretical studies. We reveal the mechanism for the rotational enhancement of the reactivity to be a strong coupling of the SiO^+ rotational mode with the reaction coordinate at the transition state on the dominant dynamical pathway.

A long-standing objective in chemistry is to control chemical reactions at the quantum level. One time-honored approach is by manipulating the collision energy (i.e., heating/cooling). This can be achieved with molecular beam techniques at collision energies ranging from cold (~1 K) to hyper-thermal (>500 K) regimes[1–4]. Recent progress in cooling atoms and molecules sheds valuable light on the quantum nature of reactivity at the single quantum state level under ultra-cold collision conditions (~nK)[5–8]. An alternative approach is to deposit energy into vibrational modes of the reactants, using for example optical pumping[9]. Such quantum state selective studies have revealed strong vibrational control in some reactions[10–12].

These investigations have led to a better understanding of how various types of energy promote (or inhibit) reactivity. Half a century ago, Polanyi proposed a set of rules for understanding the relative vibrational/translational efficacy in promoting atom-diatom reactions with different types of barriers[13]. Translational energy is more effective in overcoming a barrier that resembles the reactants (reactant-like), while vibrational excitation has a higher efficacy in surmounting a product-like barrier. These Polanyi rules have been extended to polyatomic reactions. The Sudden Vector Projection (SVP) model, for example, attributes the ability of a reactant mode in promoting a reaction to its projection onto the reaction coordinate[14,15].

Despite tremendous progress, there have only been a few experiments probing the effect of rotational excitation on reactivity, and these existing studies have typically involved only low rotational excitations[16–19]. Since rotational interval of a typical molecule is ~2 orders of magnitude smaller than vibrational intervals, the impact of rotational excitation is difficult to observe. Besides, it is not entirely clear whether a fast-rotating reactant would necessarily enhance reactivity because rotation might increase the effective barrier, hence inhibiting the reaction. In this regard, super-rotor molecules which are promoted to highly excited rotational levels are particularly useful because the energy of rotation may approach or even exceed vibrational energy or even electronic energy holding the atoms together[20,21]. Super-rotors show fascinating collisional energy exchange properties, such as a strong propensity for conservation of angular momentum

[1]Applied Physics Program, Northwestern University, Evanston 60208 IL, USA. [2]Department of Physics, Northwestern University, Evanston 60208 IL, USA. [3]Key Laboratory of Synthetic and Natural Functional Molecule of the Ministry of Education, College of Chemistry and Materials Science, Northwest University, Xi'an 710127, P. R. China. [4]Lebedev Physical Institute, Samara 443011, Russian Federation. [5]Argonne National Laboratory, Lemont 60439 IL, USA. [6]Department of Chemistry and Chemical Biology, University of New Mexico, Albuquerque 87131 NM, USA. ✉e-mail: liay@nwu.edu.cn; b-odom@northwestern.edu

(both magnitude and direction)[22], collective transport properties such as generation of macroscopic vortices[23], and anisotropic diffusion[24] and quasi-resonant vibration-rotation energy transfer[25,26].

Recently, super-rotors were detected in the interstellar medium where they may be produced by photo-dissociation of poly-atomic molecules[27] in warm proto-planetary nebulae[28] or in interstellar shock waves[29]. Due to the exotic and exceedingly diverse conditions, interstellar chemistry is very different from that on Earth. Very little is known about chemical reactions of super-rotors and their role in astrochemical reaction mechanisms.

The main focus of experimental studies on super-rotors to date has been on probing their physical[21,30] and collisional[31–33] properties using an optical molecular centrifuge[20]. The molecular centrifuge method relies on a coherent population transfer by stimulated Raman processes for the preparation of super-rotors which makes it universally applicable to many small molecules. Even though this technique is well-suited for studying collisions, the resulting relaxation dynamics make it less ideal for studying state-dependent chemical reactions.

While optically pumping trapped molecular ions is a somewhat limited approach with regard to its applicability to a wide class of molecules, it offers several advantages that make it particularly suitable for studying the reactions of super-rotors as discussed in this work. Some of the current authors recently demonstrated the state-preparation of trapped SiO^+ molecules around a target rotational state and with a narrow rotational distribution ($\Delta j = 5$)[34,35] using optical pumping. Target states can range from the ground rotational state all the way to super-rotors with 230 rotational quanta. Optical pumping is several orders of magnitude faster than any relaxational dynamics and steady-state distributions can be reached within a time scale of 1 s (Fig. 1a). Furthermore, in an ion trap, the collision rate is of the order of 1 min^{-1} which is substantially smaller than re-pump rates due to the laser. Together, they allow the study of a steady-state population.

SiO is one of the few molecules that act as a maser in the interstellar medium[36,37] and was first detected in interstellar clouds[38,39] and subsequently from supernovae explosions[40,41]. The reaction of SiO^+ with H_2 is of significance because it could play an important role in the production of interstellar SiO[42]. This was previously studied by Fahey et al. and the bi-molecular rate constant was measured to be 3.2 (1.0) × 10^{-10} cm^{-3} $molecule^{-1}$ s^{-1}[37]. We report here experimental and theoretical results on the reaction kinetics of the hydrogen abstraction reaction $SiO^+ + H_2 \rightarrow SiOH^+ + H$ in low rotational states of SiO^+ and compare it with kinetics in super-rotor states. Our experimental results indicate that rotational excitation in SiO^+ reactant enhances reactivity by a factor of 3. Theoretical calculations provide an insight into the mechanism for enhanced reactivity as well as reproduce the trend in rotational enhancement. Specifically, the enhancement is attributed to a rotational mode specificity related to a key transition state of the reaction. Implications of super-rotor reactions for astrochemistry are discussed.

Results

Reaction rates

SiO^+ ions were loaded into a room-temperature linear Paul trap via ablation followed by photo-ionization of SiO. At ultrahigh vacuum, H_2 is the background gas in the trap. Due to a large excess of H_2, $SiO^+ + H_2 \rightarrow SiOH^+ + H$ is a pseudo-first-order reaction. We use the technique of Laser Cooled Fluorescence Mass Spectrometry (LCFMS)[43,44] to measure reaction rate (see "Methods"). Given our typical Coulomb crystal size and radial trapping frequency $\Omega = 2\pi \times 240$ kHz, we expect ~10 cm^{-1} of micromotion energy for the outermost ions per degree of freedom. Assuming it is equally distributed between x, y, and z degrees of freedom, we can have up to 30 cm^{-1}, which is much less than k_bT ~ 200 cm^{-1} at 300 K. Therefore, energy of the background hydrogen gas, not the ion, dominates the collision energy for unpumped SiO^+ molecules.

The SiO^+ molecules were pumped into narrow rotational distributions centered at specified target states using an optical pumping setup (Supplementary Fig. 1). The steady-state distribution of SiO^+ and the flow of population to targeted rotational states are shown in various sub-plots in Fig. 1a-d. When SiO^+ molecules are in super-rotor states j ~ 170, the true electronic ground state is the A state (Supplementary Fig. 2b). The $X(v = 0)$ state has a very little population of SiO^+ (Fig. 1c), and nearly all the population of SiO^+ is in the A state (Fig. 1d). SiO^+ molecules are sustained in the targeted distribution limited only by their reaction with H_2. At excited rotational states, the internal

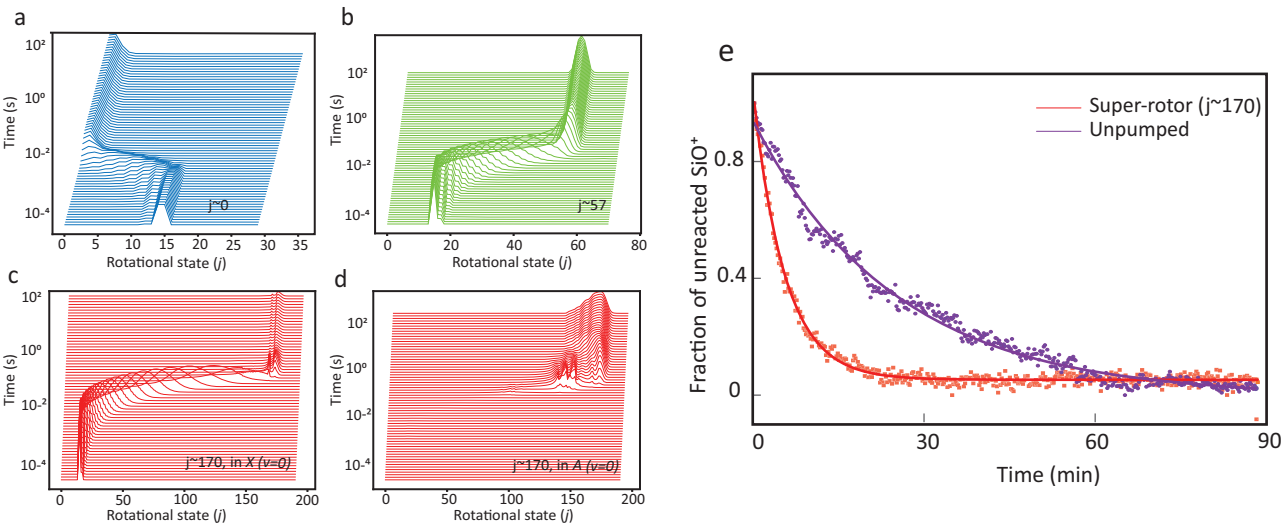

Fig. 1 | Optical pumping and reaction rate measurement. a–d The flow of SiO^+ population to the targeted rotational distribution as a function of time for which the optical pumping laser is on. As a result of the loading procedure for SiO^+ molecules in the ion trap[62], starting rotational distribution is around rotational states 13–16. The SiO^+ molecules are held in that targeted state for a long time limited only by the reaction with H_2. **e** Reaction rates for SiO^+ pumped to super-rotor states compared to an uncontrolled rotational distribution of SiO^+. The experimental data points are fit (solid lines) to an exponential decay function. A higher exponential decay constant indicates that the reaction rate is faster. The reaction rate measurement was carried out at an estimated H_2 density of 7 (1) × 10^6 cm^{-3}.

https://doi.org/10.1038/s41467-023-40135-x

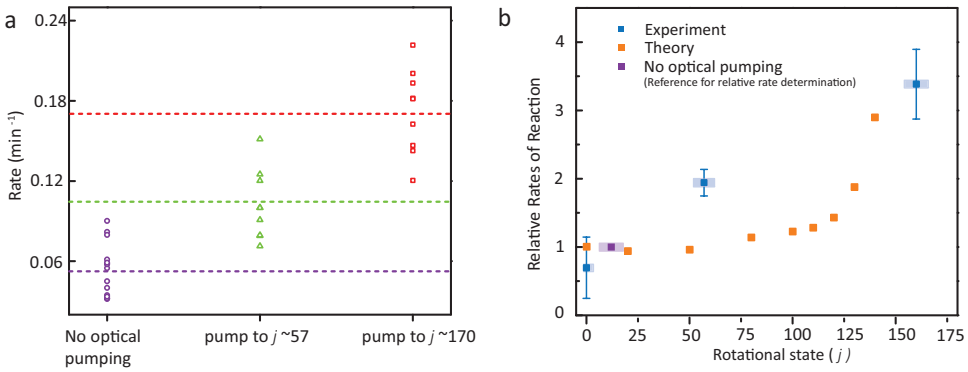

Fig. 2 | Dependence of reaction rate on rotational state. a Scatter plot showing reaction rate outcomes from repeated measurements for uncontrolled and super-rotor SiO^+. Dotted lines indicate the average of each set. All measurements were taken at the same pressure and corresponding to an estimated H_2 number density of 7 (1) × 10^6 cm^{-3}. **b** Theoretical and experimental relative rate enhancement as a function of the SiO^+ rotational quantum number. Relative experimental rates are calculated with respect to the case of no optical pumping (purple data point). Vertical error bars represent the 1σ statistical uncertainty. Horizontal error bars are the spread in prepared rotational distribution (with the spread encompassing more than 90% of the SiO^+ population). Explanations for theory calculations stopping at j=140 are discussed in the text (see section "Reaction rates").

energy of SiO^+ is ~12k_bT for $j = 57$ and ~100k_bT for $j = 170$ and completely dwarfs the energy of background H_2. Further details regarding state preparation can be found in our recent publications[34,35] and are briefly discussed in the Supplementary Information.

Figure 1e shows the fraction of unreacted SiO^+ as a function of time at an estimated H_2 number density of 7 (1) × 10^6 cm^{-3} for two cases: unpumped SiO^+ distribution and when SiO^+ molecules are pumped to super-rotor ($j = 170$) states. The super-rotors have a larger decay rate indicating a higher rate of reaction. To investigate further, we repeated the measurement several times, during which the ion gauge was constant and well within its dynamic range, and observed rates are plotted in Fig. 2a. The average pseudo-first-order rate of reaction when the SiO^+ is pumped to high j (170) super-rotor states is 0.18 (3) min^{-1} compared to 0.05 (2) min^{-1} for the case of the uncontrolled SiO^+ sample. At intermediate rotational state distribution centered at $j = 57$, a rate of 0.10 (3) min^{-1} was observed.

Theoretical enhancement in reaction rate as a function of rotational energy was calculated on the PES by a quasi-classical trajectory (QCT) method for various initial conditions. This is plotted alongside experimentally obtained results in Fig. 2b. In agreement with the experimental trend, rotational excitation of SiO^+ enhances reactivity. Quantitatively, however, calculated rate overestimates experimental values at both low and high j values. In QCT calculations, SiO^+ reactant is treated within the rigid rotor approximation, which deteriorates for large j values because of strong rotation-vibration coupling. As a result, the calculation was restricted to $j \leq 140$. Agreement between calculated and measured rate coefficients is reasonable, but not quantitative. Such levels of agreement are not uncommon for ion-molecule reactions with complex potential energy surfaces[45,46]. There are many possible theoretical reasons for the lack of quantitative agreement, chief among which is the neglect of non-adiabatic effects. Vertical excitation energy of the X to A state in SiO^+ is about 0.56 eV, which suggests possible involvement of the electronically excited state in the dynamics. Our adiabatic potential energy surface contains the lowest energy regions of the X and A states in the reactant channel (see Supplementary Fig. 6), but non-adiabatic coupling between them is ignored. Investigating non-adiabatic effects in the dynamics of the current system is an extremely challenging task and beyond the scope of the current work. In this work, we focus on the dynamical insights provided by QCT simulations on the ground adiabatic potential energy surface to understand the observed effect and its mechanistic origin, rather than a quantitative reproduction of measured rates.

Reaction mechanism

To understand reactivity and relative efficacy of various types of reactant excitation, a full-dimensional global adiabatic potential energy surface (PES) of the $SiOH_2^+(X^2A)$ system was constructed from high-level ab initio data. As shown in Fig. 3a, the PES has a complex topography, with multiple minima and saddle points. However, there is a dominant dynamics pathway leading to the abstraction of H by SiO^+. This pathway, illustrated by yellow line in Fig. 3a, features a loose pre-reaction well (IM1) with a depth of merely 0.31 eV, in which the H_2 and SiO^+ form a complex. This shallow well is nearly isotropically present around the SiO^+ moiety, suggesting an electrostatic nature. The H-abstraction saddle point (TS1) is 0.12 eV below the reactant asymptote, which features a partially broken H-H bond and an incipient H-O bond. Apparently, this reaction path is barrierless with an attractive long-range interaction, although the submerged barrier serves as a reaction bottleneck for large impact parameters. Beyond the barrier, the $SiOH^+$ product is formed exoergically.

In addition to this dominant reactive channel (the yellow pathway), there are several other channels leading to the two product asymptotes, represented in the figure by blue, red, and green lines. The formation of IM2 is blocked by a significant barrier in the entrance channel (TS0), as shown in Fig. 3a. Although access to IM3 from the reactants is barrierless (the A → D → E pathway marked in orange as shown in Fig. 3b), it is dynamically overwhelmed by a lower energy pathway A → B → C marked in cyan to the products. We have observed only a few trajectories leading to IM3 in our simulations, despite favorable energetics. Hence, these secondary reaction pathways are dynamically irrelevant. Most reactive trajectories show a striping mechanism in which the two reactants pass each other as the SiO^+ picks up the H from H_2. On the other hand, the non-reactive trajectories are usually reflected by the repulsive potential wall in close inter-monomer distances, despite the existence of stable complexes such as IM2 and IM3, as discussed above.

In Fig. 3c, the integral cross sections are plotted for three scenarios - rotational excitation of SiO^+, rotational excitation of H_2, and translational excitation. It is clear that only SiO^+ rotation promotes the reaction, while excitation in relative translation and H_2 rotation inhibits the reaction. The inhibitory effect for translational mode is due apparently to the capture nature of the reaction, while that for the H_2 rotation can be understood by the increased effective barrier with the rotational angle[15]. To explain the enhancement in reaction due to rotation of SiO^+, we resort to the SVP model[14]. In the sudden limit, the ability of a reactant mode to enhance the reactivity is attributed to a large projection of its normal mode onto the reaction coordinate at the

https://doi.org/10.1038/s41467-023-40135-x

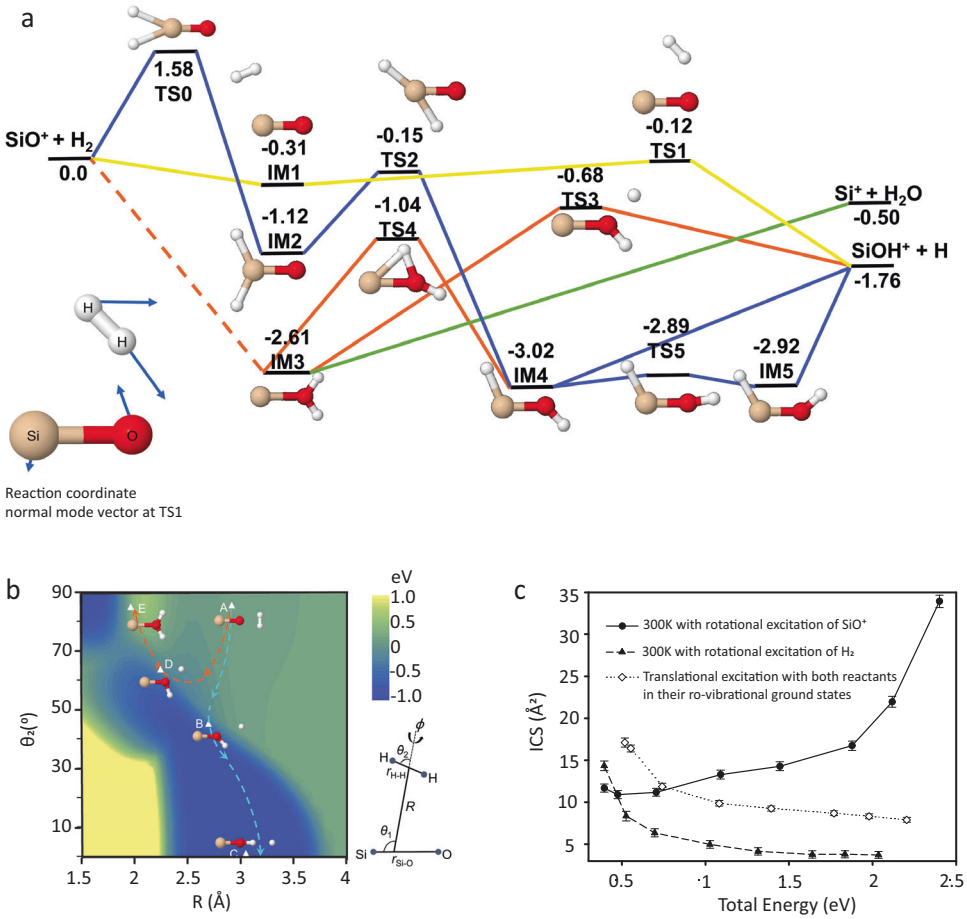

Fig. 3 | Reaction mechanism. a Energetics (in eV) of the ground state reaction pathways for the $SiO^+ + H_2$ reaction. Yellow line represents the dominant reaction pathway, via a submerged saddle point TS1. **b** Contours of the PES in reactant Jacobi coordinates along R and θ_2 with fixed $\theta_1 = 180^o$ and optimized $\mathbf{r}_{SiO}$, $\mathbf{r}_{HH}$, and ϕ. **c** Comparison of integral cross sections for rotational excitation of SiO^+, rotational excitation of H_2, and translational excitation.

relevant transition state, in this case, TS1. Table 1 lists the SVP values ($0 < \zeta_i < 1$) for all the reactant modes ($i = 1–5$); evidently, the rotation of SiO^+ has a very large value. This implies SiO^+ rotation is strongly coupled with the reaction coordinate at TS1, as illustrated in the right panel of Fig. 3a, allowing facile energy flow into the reaction coordinate.

Discussion

Optical pumping to super-rotor states provides unique opportunities for control of chemical reactions at extreme rotational energies. Preparing super-rotors with a narrow rotational distribution allows for a detailed analysis of the reaction mechanism. This work reports for the first time a chemical reaction with extreme rotational excitation of a reactant and its kinetic characterization. For the reaction $SiO^+ + H_2 \rightarrow SiOH^+ + H$, we observe an increase in the reaction rate by a factor of 3 when the SiO^+ is pumped to super-rotor states as compared to the case when we do not optically pump the SiO^+. This rotational enhancement of reactivity is supported by QCT calculations based on the newly developed PES for this reaction. Despite the complex topography of the PES, QCT calculations suggest that a submerged barrier (TS1) has an important influence on the rotational mode specificity of the reaction. The SVP model suggests that reactivity enhancement by exciting SiO^+ rotation has a contribution from strong coupling with the reaction coordinate at the dominant transition state.

Table 1 | SVP values for rotational and vibrational modes of SiO^+ and H_2 projected onto the reaction coordinate at the dominant transition state (TS1)

Mode	TS1
Rot (SiO^+)	0.42
Rot (H_2)	0.08
Vib (SiO^+)	0.05
Vib (H_2)	0.12
Translational	0.15

Extremely fast molecular rotation causes an electronic effect due to the mixing of wave functions of low-lying electronic states (such as the X and A states in SiO^+) through non-adiabatic interactions. In SiO^+ super-rotors, this effect is augmented by the centrifugal term that adds more energy to X state than to A state, resulting in closing the gap between the two states. This reverses the order of electronic states after $j = 140$ (Fig. S2) and at $j = 170$, electronic part of the wave function acquires a predominantly A state character. The electronic effect complicates studying chemical reactions of super-rotors in molecules with low-lying electronic states, such as SiO^+, and discussions on whether electronic interactions enhance or inhibit reaction rates are beyond the scope of this paper. However, this presents a future opportunity for probing the role of non-adiabatic interactions in reactive collisions by preparing ensembles of super-rotors with well-defined rotational states, i.e., by controlling the energy gap and therefore the interaction strength between the electronic states.

The observed enhancement of reaction rate may also change our understanding of chemical reactions in interstellar media (ISM). Super-rotors are known to exist in space[27–29] where they form under the action of abundant V-UV radiation on poly-atomic molecules. At the conditions in ISM, they exist for a long time, limited by radiative decay rather than collisional relaxation processes. Therefore, they can undergo reactive collisions with other ISM species. Current astro-chemical reaction models rely largely on estimated rather than measured rates, and in most cases dependence on the internal energy levels of reactants is neglected. Reactions of super rotors are an extreme example where such a chemical intuition approach fails, and a deep understanding of underlying dynamics is necessary. The observed acceleration of exoergic barrierless $SiO^+ + H_2$ reaction is counter-intuitive; similar and more significant effects may be revealed in other chemical systems with enough energy. The importance of super-rotor chemistry in ISM is determined by the interplay between rates of production by V-UV photo-dissociation, radiative relaxation, and reactive collisions. An interesting possibility is the formation of super-rotors of non-polar symmetric molecules such as H_2, O_2, and N_2, which can have several orders of magnitude longer radiative lifetime compared to polar molecules[47–50]. Therefore, they may survive for a much longer time at lower densities in interstellar media (ISM) and direct observation of rotational decays for these molecules would be very unlikely. Photo-dissociation pathways leading to the formation of non-polar symmetric molecules such as H_2[51] or CH_4[52] are known, and while such objects have not been observed yet, it is plausible that they form in super-rotor states under the action of energetic V-UV quanta on poly-atomic molecules. Even in the case of polar molecules such as OH, super-rotors can be relevant in cases such as proto-stellar clouds (where the OH super-rotors were originally discovered)[28]. Gas densities on the order of 10^{12} cm^{-3} and higher can be achieved in such environments during gravitational collapse and star formation[53]. This may be high enough for chemistry to compete with radiative cooling assuming a gas-kinetic collision rate on the order of 10^{-10} cm^{-3} s^{-1}).

Our results pave the way for studies and control of chemical reactions at extreme rotational energies of the reactants, which are important for understanding the fundamental issues in reactivity as well as chemical processes in extreme environments.

Methods

Experimental methods

SiO^+ and Ba^+ ions were co-loaded into the ion trap via ablation followed by photo-ionization. The Ba^+ cloud comprised around 500–1000 Ba^+ ions which were continuously Doppler-cooled via transitions at 493 and 650 nm. Rotational control of SiO^+ was achieved via broadband rotational optical pumping (Supplementary Information).

We applied a low-voltage (0.5–1 V) excitation chirp sweeping through frequencies from 150 to 500 kHz to one of the rods in the RF trap. As the chirp hit the secular frequency of a particular species of ions in the trap, their motion was resonantly enhanced and coupled weakly to the motion of Ba^+. This decreased the fluorescence of Ba^+ ions in proportion to the number of that ion species. A photo-multiplier tube (PMT) was used to detect the fluorescent photons from the Ba^+ cloud. A digital counter that was binned into 1 ms intervals counted the number of PMT events in each bin. As a result, each timestamp corresponded to a particular frequency over the course of one sweep. Since secular frequencies vary from one species to another as a function of their mass, this is a convenient in situ mass spectrometry technique. Besides using LCFMS as a tool to confirm the loading of SiO^+ into the trap, we also used it to monitor the reaction rate of SiO^+ with H_2. Being small, H_2 gas molecules diffuse through the vacuum chamber walls more than any other gas and therefore it is the most difficult gas to remove from the vacuum chamber. As a result, at ultra-high vacuum levels, H_2 is the dominant gas in the chamber.

As SiO^+ reacts away to form $SiOH^+$, the dip in fluorescence shifts to lower frequencies, reflecting an increase in $SiOH^+$ concentration. At any instance in time, the fluorescence spectrum is a combination of $SiOH^+$ and the unreacted SiO^+. The resolving power of LCFMS technique in our ion trap is $m/\Delta m = 30$ and thus signals from SiO^+ (44 amu) and $SiOH^+$ (45 amu) could not be resolved. Moreover, the fluorescence of Ba^+ fluctuated due to drifts in frequency, on the order of a few MHz, of the lasers used to Doppler-cool Ba^+. On rare occasions, this also led to a loss of SiO^+ ions from the trap if the drift was larger than 5 MHz. To deal with the noise from fluorescence fluctuations, we used singular value decomposition (SVD) of the data to effectively isolate amplitude variations in fluorescence from the mass-dependent frequency shift of the fluorescence spectrum. With sufficient averaging, and by appropriately employing SVD analysis, we inferred the rate of reaction of SiO^+. Refer to Supplementary Information for details on SVD analysis.

Potential energy surface and quasi-classical trajectory calculations

The global adiabatic PES for $SiOH_2^+(X^2A)$ is obtained from 20,147 ab initio points at the explicitly correlated unrestricted coupled cluster singles, doubles, and perturbative triples level of theory (UCCSD(T)-F12)[54] with the explicitly correlated correlation-consistent polarized core-valence triple-zeta basis set (pCVTZ-F12)[55], using MOLPRO[56]. These ab initio points were represented using the permutation invariant polynomial-neural network (PIP-NN) approach[57], which enforces the permutation symmetry between the two identical H nuclei. 17 PIPs[58] with the maximal order of 2 were used in the input layer of the NN, which has 2 layers with 30 and 60 and neurons in each layer. The NN training was performed using the Levenberg–Marquardt method[59] and early stop[60] was used to avoid over-fitting. The root-mean-square error (RMSE) for the best fit is 16 meV for the training set spanning the energy range of [−3.0, 7.4] eV, signaling a high-fidelity global fit of the ab initio data in the experimentally relevant energy range.

Quasi-classical trajectory (QCT) calculations were performed using the standard technique implemented in VENUS[61]. The trajectories were initiated with a 16.0 Å separation between reactants (SiO^+ and H_2), and terminated when products reach a separation of 8.0 Å, or when reactants are separated by 12.0 Å for non-reactive trajectories. In the SiO^+ rotational state-specific calculations, SiO^+ was treated as a rotating oscillator, with vibrational and rotational quantum numbers $v(=0)$ and $j(=0–140)$. Atomic coordinates and momenta of H_2 reactant were sampled randomly using a Monte Carlo approach, based on a Boltzmann distribution at 300 K. Collision energy was sampled from a Boltzmann distribution at 282 K. In the H_2 rotational state-specific calculations, H_2 was treated as a rotating oscillator with the initial state set as vibrational ground state and excited rotational states ($j = 1–14$), while SiO^+ was sampled randomly at 300 K. The maximal impact parameter of the collision was chosen as $b_{MAX} = 6.0$ Å, which was tested to be sufficient. The propagation time step was selected to be 0.05 fs, which allowed total energy conservation better than 1 meV for all trajectories. Batches of 10,000 trajectories have been run for each rotational state to make statistical errors all within 5%.

Data availability

Raw data from our experiments are available via Figshare at https://doi.org/10.6084/m9.figshare.23639526.

References

1. Brunsvold, A. L. et al. Dynamics of hyperthermal collisions of $O(^3P)$ with CO. *J. Phys. Chem. A* **112**, 2192–2205 (2008).
2. Dong, W. et al. Transition-state spectroscopy of partial wave resonances in the F + HD reaction. *Science* **327**, 1501–1502 (2010).
3. Pan, H., Wang, F., Czakó, G. & Liu, K. Direct mapping of the angle-dependent barrier to reaction for Cl + CHD_3 using polarized scattering data. *Nat. Chem.* **9**, 1175–1180 (2017).

4. Yang, T. et al. Enhanced reactivity of fluorine with para-hydrogen in cold interstellar clouds by resonance-induced quantum tunnelling. *Nat. Chem.* **11**, 744–749 (2019).
5. Ni, K.-K. et al. Dipolar collisions of polar molecules in the quantum regime. *Nature* **464**, 1324–1328 (2010).
6. Ospelkaus, S. et al. Quantum-state controlled chemical reactions of ultracold potassium-rubidium molecules. *Science* **327**, 853–857 (2010).
7. Hu, M.-G. et al. Direct observation of bimolecular reactions of ultracold KRb molecules. *Science* **366**, 1111–1115 (2019).
8. Liu, Y. et al. Precision test of statistical dynamics with state-to-state ultracold chemistry. *Nature* **593**, 379–384 (2021).
9. Zare, R. N. Laser control of chemical reactions. *Science* **279**, 1875–1879 (1998).
10. Bronikowski, M. J., Simpson, W. R., Girard, B. & Zare, R. N. Bond-specific chemistry: OD:OH product ratios for the reactions H +HOD(100) and H+HOD(001). *J. Chem. Phys.* **95**, 8647–8648 (1991).
11. Sinha, A., Hsiao, M. C. & Crim, F. F. Controlling bimolecular reactions: mode and bond selected reaction of water with hydrogen atoms. *J. Chem. Phys.* **94**, 4928–4935 (1991).
12. Yan, S., Wu, Y.-T., Zhang, B., Yue, X.-F. & Liu, K. Do vibrational excitations of CHD_3 preferentially promote reactivity toward the chlorine atom? *Science* **316**, 1723–1726 (2007).
13. Polanyi, J. C. Some concepts in reaction dynamics. *Science* **236**, 680–690 (1987).
14. Guo, H. & Jiang, B. The sudden vector projection model for reactivity: mode specificity and bond selectivity made simple. *Acc. Chem. Res.* **47**, 3679–3685 (2014).
15. Jiang, B., Li, J. & Guo, H. Effects of reactant rotational excitation on reactivity: perspectives from the sudden limit. *J. Chem. Phys.* **140**, 034112 (2014).
16. Liu, X., Wang, C. C., Harich, S. A. & Yang, X. Effect of a single quantum rotational excitation on state-to-state dynamics of the O(1D) + H2 → OH + H reaction. *Phys. Rev. Lett.* **89**, 133201 (2002).
17. Xu, Y., Xiong, B., Chang, Y. C. & Ng, C. Y. Communication: Rovibrationally selected absolute total cross sections for the reaction $H_2O^+(X^2B_1; v_1^+ v_2^+ v_3^+ = 000; n_{Ka+Kc+}^+) + D_2$: observation of the rotational enhancement effect. *J. Chem. Phys.* **137**, 241101 (2012).
18. Shagam, Y. et al. Molecular hydrogen interacts more strongly when rotationally excited at low temperatures leading to faster reactions. *Nat. Chem.* **7**, 921 (2015).
19. Wang, F., Pan, H. & Liu, K. Imaging the effect of reactant rotations on the dynamics of the $Cl + CHD_3(v_1 = 1, |J,K\rangle)$ reaction. *J. Phys. Chem. A* **119**, 11983–11988 (2015).
20. Karczmarek, J., Wright, J., Corkum, P. & Ivanov, M. Optical centrifuge for molecules. *Phys. Rev. Lett.* **82**, 3420–3423 (1999).
21. Korobenko, A., Milner, A. A. & Milner, V. Direct observation, study, and control of molecular superrotors. *Phys. Rev. Lett.* **112**, 113004 (2014).
22. Hay, S., Shokoohi, F., Callister, S. & Wittig, C. Collisional metastability of high rotational states of CN ($X^2\Sigma^+$, v″= 0). *Chem. Phys. Lett.* **118**, 6–11 (1985).
23. Steinitz, U., Prior, Y. & Averbukh, I. S. Laser-induced gas vortices. *Phys. Rev. Lett.* **109**, 033001 (2012).
24. Khodorkovsky, Y., Steinitz, U., Hartmann, J.-M. & Averbukh, I. S. Collisional dynamics in a gas of molecular super-rotors. *Nat. Commun.* **6**, 7791 (2015).
25. Magill, P. D., Stewart, B., Smith, N. & Pritchard, D. E. Dynamics of quasiresonant vibration-rotation transfer in atom-diatom scattering. *Phys. Rev. Lett.* **60**, 1943–1946 (1988).
26. Stewart, B., Magill, P. D., Scott, T. P., Derouard, J. & Pritchard, D. E. Quasiresonant vibration ↔ rotation transfer in atom-diatom collisions. *Phys. Rev. Lett.* **60**, 282–285 (1988).
27. Chang, Y. et al. Electronically excited oh super-rotors from water photodissociation by using vacuum ultraviolet free-electron laser pulses. *J. Phys. Chem. Lett.* **11**, 7617–7623 (2020).
28. Carr, J. S. & Najita, J. R. The OH rotational population and photodissociation of H_2O in DG tauri. *Astrophys. J.* **788**, 66 (2014).
29. Tappe, A., Lada, C. J., Black, J. H. & Muench, A. A. Discovery of superthermal hydroxyl (OH) in the HH 211 outflow. *Astrophys. J.* **680**, 117–120 (2008).
30. Korobenko, A., Hepburn, J. W. & Milner, V. Observation of non-dispersing classical-like molecular rotation. *Phys. Chem. Chem. Phys.* **17**, 951–956 (2015).
31. Murray, M. J., Ogden, H. M. & Mullin, A. S. Anisotropic kinetic energy release and gyroscopic behavior of CO_2 super rotors from an optical centrifuge. *J. Chem. Phys.* **147**, 154309 (2017).
32. Murray, M. J., Ogden, H. M. & Mullin, A. S. Importance of rotational adiabaticity in collisions of CO_2 super rotors with Ar and He. *J. Chem. Phys.* **148**, 084310 (2018).
33. Murray, M. J., Ogden, H. M., Toro, C., Liu, Q. & Mullin, A. S. Impulsive collision dynamics of CO super rotors from an optical centrifuge. *ChemPhysChem* **17**, 3692–3700 (2016).
34. Stollenwerk, P. R., Antonov, I. O., Venkataramanababu, S., Lin, Y.-W. & Odom, B. C. Cooling of a zero-nuclear-spin molecular ion to a selected rotational state. *Phys. Rev. Lett.* **125**, 113201 (2020).
35. Antonov, I. O. et al. Precisely spun super rotors. *Nat. Commun.* **12**, 2201 (2021).
36. Elitzur, M. in *Interstellar Processes* (eds Hollenbach, D. J. & Thronson, H. A.) 762–780 (Springer, 1987).
37. Fahey, D., Fehsenfeld, F., Ferguson, E. & Viehland, L. Reactions of Si^+ with H_2O and O_2 and SiO^+ with H_2 and D_2. *J. Chem. Phys.* **75**, 669–674 (1981).
38. Rubin, R. H., Swenson, J. G. W., Benson, R. C., Tigelaar, H. L. & Flygare, W. H. Microwave detection of interstellar formamide. *Astrophys. J.* **169**, 39 (1971).
39. Langer, W. D. & Glassgold, A. E. Silicon chemistry in interstellar clouds. *Astrophys. J.* **352**, 123 (1990).
40. Liu, W. & Dalgarno, A. Formation and destruction of silicon monoxide in SN 1987a. *Astrophys. J.* **471**, 480–484 (1996).
41. Aitken, D. K. et al. 10 μm spectral observations of SN 1987A: interpretation of the infrared excess. *Mon. Not. R. Astron. Soc.* **231**, 7–14 (1988).
42. Turner, J. & Dalgarno, A. The chemistry of silicon in interstellar clouds. *Astrophys. J.* **213**, 386–389 (1977).
43. Baba, T. & Waki, I. Laser-cooled fluorescence mass spectrometry using laser-cooled barium ions in a tandem linear ion trap. *J. Appl. Phys.* **89**, 4592–4598 (2001).
44. Baba, T. & Waki, I. Cooling and mass-analysis of molecules using laser-cooled atoms. *Jpn. J. Appl. Phys.* **35**, 1134 (1996).
45. Yang, T. et al. Optical control of reactions between water and laser-cooled Be^+ ions. *J. Phys. Chem. Lett.* **9**, 3555–3560 (2018).
46. Kumar, S. S., Grussie, F., Suleimanov, Y. V., Guo, H. & Kreckel, H. Low temperature rates for key steps of interstellar gas-phase water formation. *Sci. Adv.* **4**, 3417 (2018).
47. Bruna, P. J. & Grein, F. The $a^2\Pi_u$ state of N_2^+: electric properties, fine and hyperfine coupling constants, and magnetic moments (g-factors). a theoretical study. *J. Mol. Spectrosc.* **250**, 75–85 (2008).
48. Najafian, K., Meir, Z. & Willitsch, S. From megahertz to terahertz qubits encoded in molecular ions: theoretical analysis of dipole-forbidden spectroscopic transitions in N_2^+. *Phys. Chem. Chem. Phys.* **22**, 23083–23098 (2020).
49. Germann, M. Dipole-forbidden vibrational transitions in molecular ions. PhD thesis, Univ. Basel (2016).
50. Herzberg, G. *Molecular Spectra and Molecular Structure. Spectra of Diatomic Molecules*, Vol. 1, 2nd edn (Van Nostrand Reinhold, 1950).

51. Chambreau, S. D., Lahankar, S. A. & Suits, A. G. Correlated v_{H2} and j_{CO} product states from formaldehyde photodissociation: dynamics of molecular elimination. *J. Chem. Phys.* **125**, 044302 (2006).
52. Zhao, Y.-L., Laufer, A. H., Halpern, J. B. & Fahr, A. Hydrogen migration and vinylidene pathway for formation of methane in the 193 nm photodissociation of propene: CH_3CHCH_2 and CD_3CDCD_2. *J. Phys. Chem. A* **111**, 8330–8335 (2007).
53. Podio, L. et al. Water vapor in the protoplanetary disck of DG Tau. *Astrophys. J. Lett*. (2013).
54. Knizia, G., Adler, T. B. & Werner, H.-J. Simplified CCSD(T)-F12 methods: theory and benchmarks. *J. Chem. Phys.* **130**, 054104 (2009).
55. Pritchard, B. P., Altarawy, D., Didier, B., Gibson, T. D. & Windus, T. L. New basis set exchange: an open, up-to-date resource for the molecular sciences community. *J. Chem. Inf. Model.* **59**, 4814–4820 (2019).
56. Werner, H. et al. MOLPRO, version 2015.1, a package of ab initio programs, 2015 (University of Cardiff Chemistry Consultants (UC3), 2017).
57. Jiang, B., Li, J. & Guo, H. Potential energy surfaces from high fidelity fitting of ab initio points: the permutation invariant polynomial - neural network approach. *Int. Rev. Phys. Chem.* **35**, 479–506 (2016).
58. Braams, B. J. & Bowman, J. M. Permutationally invariant potential energy surfaces in high dimensionality. *Int. Rev. Phys. Chem.* **28**, 577–606 (2009).
59. Hagan, M. T. & Menhaj, M. B. Training feedforward networks with the Marquardt algorithm. *IEEE Trans. Neural Net.* **5**, 989–993 (1994).
60. Raff, L., Komanduri, R., Hagan, M. & Bukkapatnam, S. *Neural Networks in Chemical Reaction Dynamics* (Oxford University Press, 2012).
61. Hu, X., Hase, W. L. & Pirraglia, T. Vectorization of the general Monte Carlo classical trajectory program venus. *J. Comp. Chem.* **12**, 1014–1024 (1991).
62. Stollenwerk, P. R., Antonov, I. O. & Odom, B. C. IP determination and 1+ 1 REMPI spectrum of SiO at 210–220 nm in an ion trap: implications for SiO^+ ion trap loading. *J. Mol. Spectrosc.* **355**, 40–45 (2019).

Acknowledgements

Development of dissociative analysis techniques were funded by NSF Grant No. PHY-1806861, and super rotor pumping techniques and chemistry analysis were supported by AFOSR Grant No. FA9550-17-1-0352. A.L. would like to thank the National Science Foundation of China (Grant No. 22073073) and Natural Science Basic Research Plan in Shaanxi Province of China (Grant No. 2021JM-311), and H.G. thanks the AFOSR for financial support (Grant No. FA9550-22-1-0350).

Author contributions

S.V., I.A., and P.S. developed the laboratory techniques. S.V., J.D., I.A., and P.S. took data. B.O. led the experimental effort. A.L. and H.G. performed the theoretical calculations.

Competing interests

The authors declare no competing interests.

Additional information

Supplementary information The online version contains supplementary material available at https://doi.org/10.1038/s41467-023-40135-x.

Correspondence and requests for materials should be addressed to Anyang Li or Brian C. Odom.

Peer review information *Nature Communications* thanks Matthew Murray and the anonymous reviewer(s) for their contribution to the peer review of this work. A peer review file is available.